Sub-10 nm Scale Microphase Separation in Star-Block Copolymers Consisting of Maltotriose and Poly(ε-caprolactone)

Takuya Isono,[1,*] Nao Kwakami,[2] Kodai Watanabe,[2] Kohei Yoshida,[2] Hiroaki Mamiya,[3] and Toshifumi Satoh[1]

[1]Division of Applied Chemistry, Faculty of Engineering, Hokkaido University
Kita-13, Nishi-8, Kita-ku, Sapporo, 060-8628, Japan
[2]Graduate School of Chemical Sciences and Engineering, Hokkaido University
Kita-13, Nishi-8, Kita-ku, Sapporo, 060-8628, Japan
[3]National Institute for Materials Science
1-2-1, Sengen, Tsukuba, 305-0047, Japan

1 Introduction

Microphase separation of block copolymers (BCPs) has attracted much attention for its application in nanolithographic applications [1]. Thus, creating BCPs capable of forming microphase-separated structures with smaller domain-spacing, especially less than 10 nm, is of particular importance. To achieve such smaller domain-spacing, the BCP needs to possess both high Flory-Huggins interaction (χ) parameter and low degree of polymerization (N). Our group has recently been focusing on the design of the high χ-low N BCPs by employing oligosaccharide as one of the block components [2-4]. The strong hydrophilic character and rigid structure of the oligosaccharide segment enable the oligosaccharide-based BCPs to microphase separate even at very low N region, leading to the ordered nanostructures with domain-spacing around 10 nm. However, the low N of such BCPs (typically, a few thousand) would cause many issues including a lower glass transition temperature, lower viscosity, less film formability, and reduced mechanical properties, which eventually made the BCPs unusable in nanofabrication applications.

In this study, we turned our attention to apply star-block architecture to the oligosaccharide-based BCP. Most interesting feature of $(AB)_x$ star-block architecture is that they show the same morphology and domain-spacing value in the microphase-separated structures as the constitutional AB diblock arm [5]. This means that the domain-spacing can be fixed despite an increase in the total molecular weight with the increasing arm number. Thus, integrating high χ BCP molecules into a star-block copolymer could be a new solution to simultaneously enable the sub-10 nm scale microphase separation and improve the molecular weight. Herein, we investigated the microphase separation behaviors of three-, four-, and six-armed star-block copolymers composed of poly(ε-caprolactone) (PCL) and maltotriose (MT), i.e., (PCL-b-MT)₃, (PCL-b-MT)₄, and (PCL-b-MT)₆, respectively (Figure 1).

2 Experiment

According to our previous synthetic scheme, the star-block copolymers, (PCL-b-MT)$_x$, were synthesized through three step reactions involving ring-opening polymerization of ε-caprolactone, end-functionalization, and click reaction [6]. The molecular characteristics of the star-block copolymers and the linear counterparts (PCL-b-MT) are summarized in Table 1.
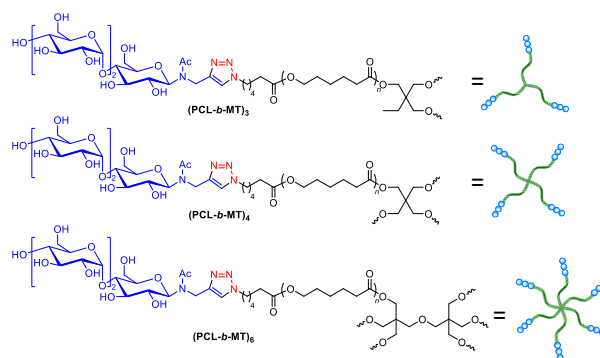

Figure 1. Chemical structure of (PCL-b-MT)$_x$ star-block copolymers (x = 3, 4, and 6).

Table 1. Molecular characteristics of PCL-b-MT linear deblock copolymer and (PCL-b-MT)$_x$ star-block copolymers

	$M_{n,NMR}$[a] (g mol⁻¹)	M_w/M_n[b]	Φ_{MT}[c]
PCL-b-MT	3500	1.08	0.14
(PCL-b-MT)₃	8900	1.10	0.15
(PCL-b-MT)₄	11400	1.11	0.17
(PCL-b-MT)₆	15600	1.10	0.17

[a]Determined by ¹H NMR in DMSO-d_6. [b]Determined by SEC in DMF containing 0.01 M LiCl using polystyrene standards. [c]MT volume fraction (Φ_{MT}) was calculated based on the known density value for the blocks: 1.15 g cm⁻³ for PCL and 1.36 g cm⁻³ for amylose (instead of MT).

The small-angle and wide-angle X-ray scattering (SAXS/WAXS) measurements were conducted on the powder samples at BL-6A in PF. The BCP sample was put into a glass capillary. The SAXS and WAXS profiles were obtained by 20 °C step during the step-by-step cooling process from the molten state (140 °C) to -20 °C with the INSTEC temperature controller (cooling rate, 5 °C min⁻¹; λ = 1.50 Å; acquisition time, 30 sec), in which each scan

was started just after holding the desired temperature for 1 min. The GISAXS experiments were conducted on the BCP thin films on a silicon wafer at BL-6A in PF (λ = 1.50 Å; acquisition time, 10 sec).

3   Results and Discussion

To observe the microphase-separated structures in the linear and star-block copolymers, we performed the SAXS measurements on the powder samples. Initially, the samples were heated at 140 °C, then the SAXS profiles were acquired at this temperature. All the samples showed the scattering pattern corresponding to the hexagonally close-packed cylindrical structure (Figure 2). The domain-spacing, $d = 2\pi/q^*$, was calculated to be 7.9 nm for PCL-*b*-MT, 8.6 nm for (PCL-*b*-MT)$_3$, 7.5 nm for (PCL-*b*-MT)$_4$, and 7.6 nm for (PCL-*b*-MT)$_6$. These results confirmed that the arm number in the star-block copolymers had small impact on the resulting morphology and domain-spacing.
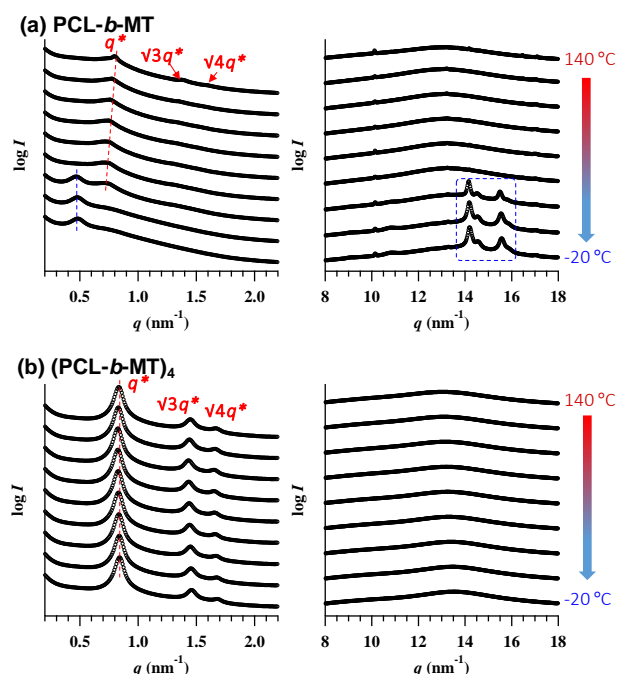

Figure 2. Changes in SAXS (left) and WAXS profiles (right) of (a) PCL-*b*-MT and (b) (PCL-*b*-MT)$_4$ during the step-by-step cooling from 140 to -20 °C.

Next, SAXS and WAXS profiles were acquired during the cooling process from 140 to -20 °C. Figure 2 shows the SAXS and WAXS results for PCL-*b*-MT and (PCL-*b*-MT)$_4$ as the representative examples. No apparent change was observed both in the SAXS and WAXS profiles for the star-block copolymers even after cooling to -20 °C. This suggests that the ordered microphase-separated structure formed in the molten state was preserved even after the cooling. In addition, no evidence of the PCL crystallization was observed in the WAXS profiles of the star-block copolymers throughout the cooling process. On the other hand, for the linear diblock copolymer, the scattering peak at around q of ca. 0.8 nm^{-1} due to the microphase separation diminished with decreasing temperature, and eventually disappeared at around 0 °C. At the same time, a new

scattering peak at q of ca. 0.4 nm^{-1} newly appeared at below 20 °C, which might be attributed to the crystalline-amorphous lamellar for the PCL domain. The emergence of the scattering peaks due to the PCL crystal (q = 14.2, 14.6, 15.6 nm^{-1} corresponding to [110], [111], and [200] planes) were observed in the WAXS profiles obtained at below 20 °C. Therefore, in the case of the linear diblock copolymer, the microphase-separated structure formed in the molten state was destroyed during the cooling process because of the rapid crystallization of the PCL block. Based on the SAXS and WAXS experiments, we found that the star-block architecture has the benefit of regulating the crystallization behavior of the PCL block, leading to ordered microphase-separated structures in the bulk state.

Next, we investigated the microphase separation behaviors in the thin film state by grazing incidence SAXS (GISAXS) measurements. The thin film samples were prepared by spin-coating the polymer solution onto a hydrophilic silicon wafer followed by thermal annealing at 130 °C for 30 min under vacuum. Figure 3 shows the GISAXS images for PCL-*b*-MT and (PCL-*b*-MT)$_4$ as the representative examples. The PCL-*b*-MT thin film showed a featureless scattering profile in the GISAXS image, suggesting the poor ordering even in the thin film state. On the other hand, all the star-block copolymer thin films showed scattering patterns corresponding to the horizontally orientated nanostructures in their GISAXS images. The difference in the thin film morphology can also be explained by the crystallization of the PCL block: the rapid PCL crystallization in the linear diblock copolymer interfered with the microphase separation in the thin film state during the cooling process.
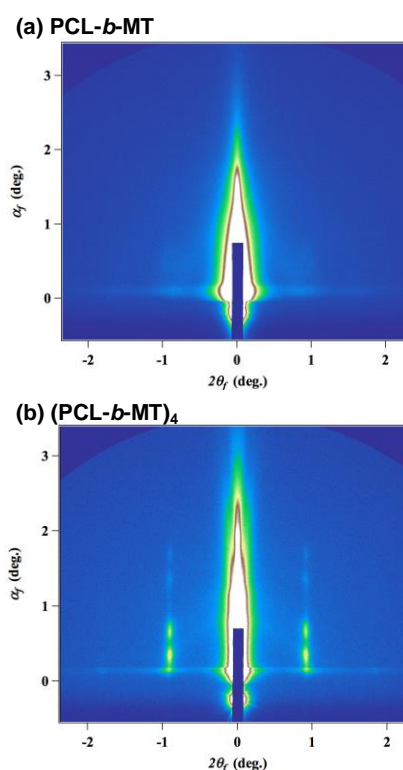

Figure 3. GISAXS images of (a) PCL-*b*-MT and (b) (PCL-*b*-MT)$_4$ thin films annealed at 130 °C for 30 min.

4 Conclusion

In the molten state, the star-block copolymers, i.e., (PCL-*b*-MT)$_x$ (x = 3, 4, and 6), and their linear diblock counterpart, i.e., PCL-*b*-MT, showed hexagonally close-packed cylindrical structures with the domain-spacing of around 8 nm. Importantly, the morphology and domain-spacing were essentially the same regardless of the arm number. The arm length and MT volume fraction determined the resulting microphase-separated structures. Thus, we succeeded in obtaining extremely small nanostructures from the BCPs with the molecular weight of higher than 10000 g mol^{-1}. Furthermore, we found that the star-block architecture regulate the PCL crystallization behavior of (PCL-*b*-MT)$_x$, which was beneficial to fabricate the ordered nanostructures in both the bulk and thin film states after the thermal annealing process.

References
[1] S.-J. Jeong, et al., Mater. Today **16**, 469 (2013).
[2] T. Isono, et al., J. Photopolym. Sci. Technol. **28**, 635 (2015).
[3] I. Otsuka, et al., Macromolecules **48**, 1509 (2015).
[4] T. Isono, et al., Macromolecules **51**, 428 (2018)
[5] K. Ishizu and S. Uchida, Prog. Polym. Sci. **24**, 1439 (1999).
[6] T. Isono, et al., Macromolecules **46**, 8932 (2013).

Research Achievements
1. T. Isono, et al., Polym. Chem. **10**, 1119 (2019).

* isono.t@eng.hokudai.ac.jp